EPJ Nuclear
Sciences
& Technologies

Available online at:
https://www.epj-n.org

REGULAR ARTICLE

Using effective temperature as a measure of the thermal scattering law uncertainties to UOX fuel calculations from room temperature to 80°C

Gilles Noguere[*] and Shuqi Xu

CEA, DES, IRESNE, DER, Cadarache 13108 Saint Paul Les Durance, France

Abstract. The effective temperature T_{eff} is an important physical quantity in neutronic calculations. It can be introduced in a Free Gas Model to approximate crystal lattice effects in the Doppler broadening of the neutron cross sections. In the last decade, a few research works proposed analytical or Monte-Carlo perturbation schemes for estimating uncertainties in neutronic calculations due to thermal scattering laws. However, the relationship between the reported results with T_{eff} was not discussed. The present work aims to show how the effective temperature can measure the impact of the thermal scattering law uncertainties on neutronic calculations. The discussions are illustrated with Monte-Carlo calculations performed with the TRIPOLI-4® code on the MISTRAL-1 benchmark carried out in the EOLE facility of CEA Cadarache (France) from room temperature to 354 K (80°C). The uncertainty analysis is focused on the impact of the thermal scattering laws of H_2O and UO_2 on the neutron multiplication factor k_{eff} for UOX fuel moderated by water. When using the H_2O and UO_2 candidate files for the JEFF-4 library, the variation range of T_{eff} leads to a k_{eff} uncertainty of 2.3 pcm/K, on average. In the temperature range investigated in this work, T_{eff} uncertainties of ±20 K for H_2O and ±10 K for UO_2 give uncertainties on the multiplication factor that remains close to ±50 pcm. Such a low uncertainty confirms the improved accuracy achieved on the modelisation of the latest thermal scattering laws of interest for light water reactors. In the future evaluated nuclear data libraries, uncertainty budget analysis associated with the low neutron energy scattering process will be a marginal contribution compared to the capture process.

1 Introduction

The propagation of the thermal scattering law uncertainties to neutron cross sections and neutronic parameters is addressed in a few works reported in the literature. Methodologies rely on Monte-Carlo or direct perturbations of the model parameters involved in the calculation of the thermal scattering laws. Owing to its importance for criticality and reactor applications, they were mainly applied to H_2O [1–7]. The present work aims to complement the reported results by including the effects of the thermal scattering laws of UO_2.

Part of the model parameters used in the description of the elastic scattering cross section at low neutron energies comes from abinitio or molecular dynamic simulations. Therefore, the relationship between condensed matter and neutronic physics is not straightforward. Several calculation steps handled by dedicated processing tools are needed to link the model parameters and the neutronic parameters. In the case of UOX integral benchmarks with UO_2 fuel moderated by water, this relationship can be simplified by assuming some approximations. The originality of this work is to use the effective temperature as an uncertainty indicator for quantifying the impact of the thermal scattering laws on the neutron multiplication factor. The effective temperature has the advantage of taking into account the vibration dynamics or atom binding effects of materials [8–11], but neglects some complex molecular behaviour, such as in the case of the water molecule. Fortunately, this specificity of the water molecule plays a minor role in the uncertainty quantification process associated to UOX benchmarks [4].

In this study, the relevance of using the effective temperature as an uncertainty indicator is illustrated with the MISTRAL-1 benchmarks [12] carried out at the EOLE facility (CEA Cadarache, France). The neutron multiplication factor was measured as a function of temperature up to 354 K (80°C). Such a unique set of integral results is suitable for testing the relationship between the effective temperature and the thermal scattering laws of H_2O and UO_2. For this purpose, the nominal calculations were performed with the Monte-Carlo code TRIPOLI-4® [13] by

* e-mail: gilles.noguere@cea.fr

Table 1. Effective temperatures calculated with the H_2O and UO_2 candidate files for the JEFF-4 library, which is available in the test library JEFF-4T1.

Temperature	294 K	354 K
$T_{\rm eff}$ for ^{1}H in H_2O	1195 K	1208 K
$T_{\rm eff}$ for ^{238}U in UO_2	311 K	369 K
$T_{\rm eff}$ for ^{16}O in UO_2	378 K	425 K

using the evaluated nuclear data library JEFF-3.1.1. The perturbed calculations also rely on JEFF-3.1.1 in which the thermal scattering laws of H_2O and UO_2 were replaced by candidate files for the JEFF-4 library, which are available in the test library JEFF-4T1 [14].

The definition of the effective temperature is given in Section 2. Section 3 presents the methodology used to propagate the model parameter uncertainties of the thermal scattering laws to the neutron multiplication factor in the case of the MISTRAL-1 core. Uncertainties obtained on the neutron cross sections of H_2O and UO_2, as well as their contributions on the $k_{\rm eff}$ uncertainty are discussed in Section 4.

2 Effective temperature

The evaluated nuclear data files used in this work come from the working library JEFF-4T1, which contains new files for H_2O and UO_2. The evaluation of ^{1}H in H_2O is a slightly modified version of the file available in the US library (ENDF/B.VIII.0) [15]. The evaluation was modified to include a refined temperature grid, including the freezing point (273.15 K), critical point (674.1 K), and a grid with 5 K interval between 285 K and 650 K. Extrapolated temperature points between 650 K and 1000 K (every 50 K) were also added. The model relies on a Gaussian expansion, following the work of Maul et al. [4]. The evaluations for ^{238}U and ^{16}O in UO_2 are based on experimental results measured at the Institute Laue-Langevin of Grenoble (France). Detailed explanations are given in references [16,17]. The evaluated nuclear data files for UO_2 contain thermal scattering laws for 31 temperatures ranging from 284 K to 1700 K.

The CINEL code [18] was used to generate the thermal scattering laws for H_2O and UO_2 by starting from model parameters describing the dynamics and structure of the materials. The key parameter is the phonon density of states $\rho(\omega)$, from which the effective temperature is calculated as follows [9,19]:

$$T_{\rm eff} = \frac{\hbar}{2k_{\rm B}} \int_0^\infty \omega \rho(\omega) \coth\left(\frac{\hbar\omega}{2k_{\rm B}T}\right) {\rm d}\omega, \qquad (1)$$

where T is the temperature of the material under consideration, $k_{\rm B}$ represents the Boltzmann constant and $\hbar\omega$ stands for the neutron energy transfer. The effective temperatures at $T = 294$ K (20°C) and $T = 354$ K (80°C) are listed in Table 1.
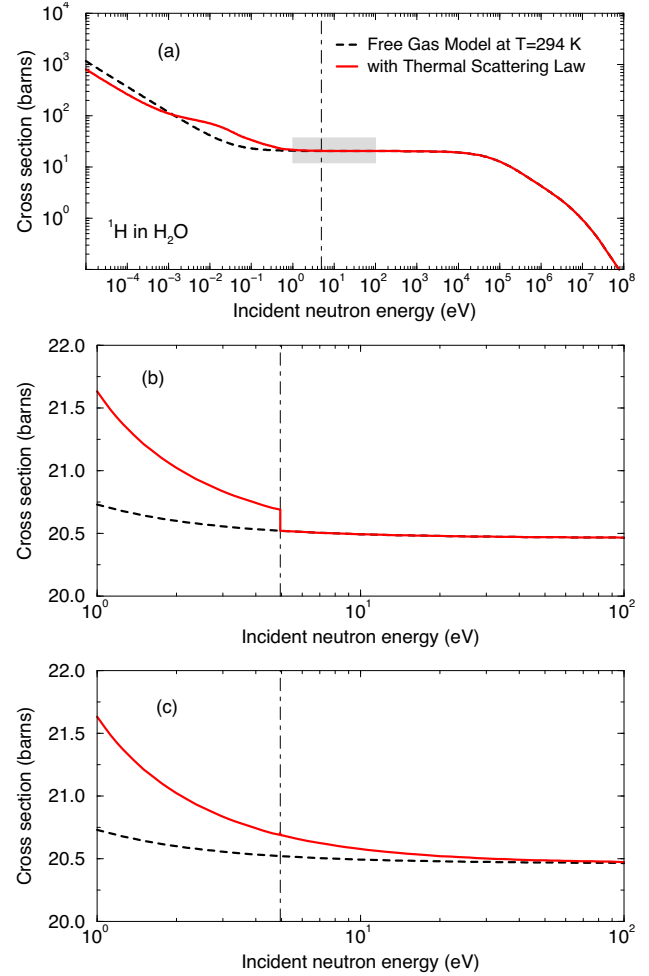

Fig. 1. Elastic scattering cross section of ^{1}H in H_2O as a function of the neutron incident energy. The top plot (a) shows the neutron cross-section over the full energy range. The middle plot (b) highlights the discontinuity at the thermal cut-off energy (4.95 eV) between the thermal scattering law and the Free Gas Model when the thermodynamic temperature T is introduced in the Free Gas Model. The bottom plot (c) shows the continuous behaviour of the cross-section when $T = T_{\rm eff}$.

For ^{1}H in H_2O, the importance of the effective temperature can be illustrated by the behaviour of the elastic scattering cross section around the thermal cut-off energy of 4.95 eV (Fig. 1). Above this energy, nuclear data processing codes use a Free Gas Model to reconstruct the neutron cross sections at a given temperature T. A continuous behaviour between the thermal scattering law and the Free Gas Model treatments can only be achieved by introducing $T = T_{\rm eff}$ in the Free Gas Model.

For UO_2, the effective temperature is related to the Doppler broadening of the ^{238}U resonances. As shown in Figure 2, the first resonance of ^{238}U is very close to the thermal cut-off energy of 4 eV, below which dominate the different components of the elastic scattering of ^{238}U and ^{16}O in UO_2. For reactor applications, it is useful to link the effective and Debye temperatures $\theta_{\rm D}$ by introducing a Debye phonon spectrum in equation (1). The first-order
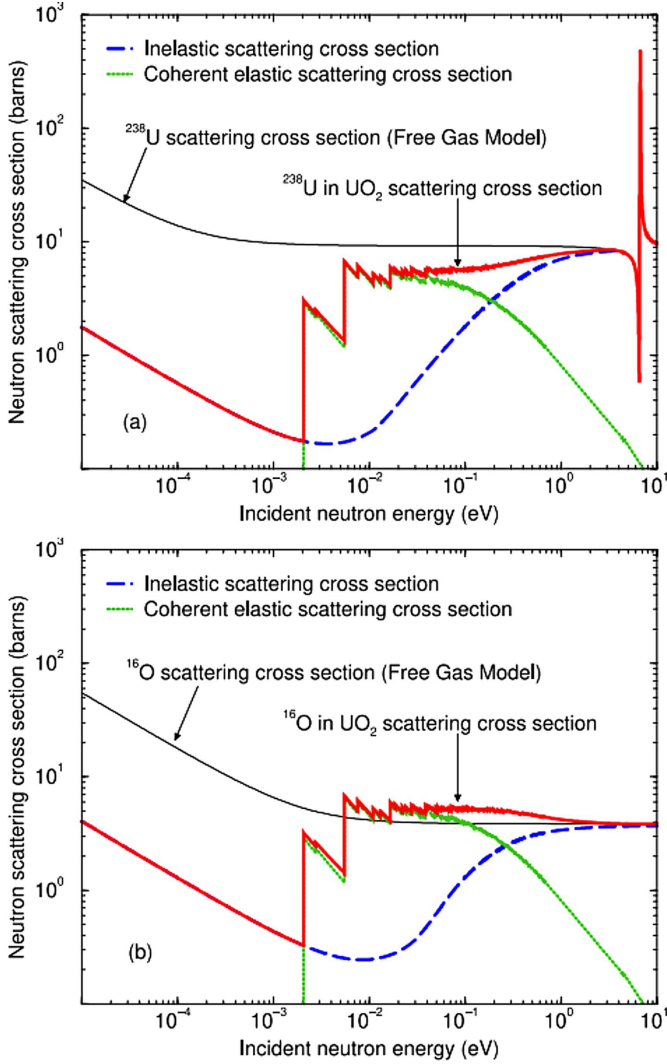
Fig. 2. Neutron elastic scattering cross sections of ^{238}U and ^{16}O in UO$_2$ reconstructed with the evaluated nuclear data files available in the test library JEFF-4T1.

approximation leads to:

$$\frac{T_{\mathrm{eff}}}{T} = 1 + \frac{1}{20}\left(\frac{\theta_{\mathrm{D}}}{T}\right)^2. \tag{2}$$

Butland [20] derived a similar expression by introducing a phonon density of states for ^{238}U in UO$_2$ calculated by Thorson and Jarvis:

$$\left(\frac{T_{\mathrm{eff}}}{T}\right)_{\mathrm{B}} = 1 + \frac{3110}{T^2}. \tag{3}$$

The combination of equations (2) and (3) gives a Debye temperature of $\theta_{\mathrm{D}} = 249$ K, which is equal to the Debye temperature reported in reference [21] derived from specific heat measurements at low temperature.

Starting from the work of Butland, Meister [22] approximated the phonon density of states of ^{238}U in UO$_2$ by an Einstein model with acoustic and optical vibration
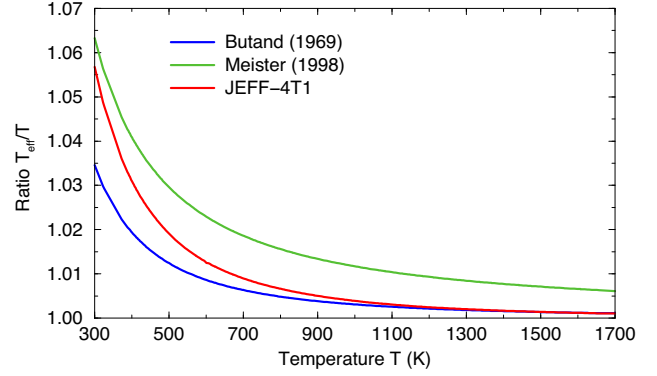

Fig. 3. Ratio T_{eff}/T for ^{238}U in UO$_2$ calculated with equations (3), (4) and (1) as a function of T.

modes, whose characteristics were deduced from transmission experiments performed at the GELINA facility [23]. Equivalences between effective resonance integrals calculated with Free Gas and Crystal Lattice Model provided the following parameterization:

$$\left(\frac{T_{\mathrm{eff}}}{T}\right)_{\mathrm{M}} = \left(\frac{T_{\mathrm{eff}}}{T}\right)_{\mathrm{B}} + \frac{8.6}{T}. \tag{4}$$

According to this expression, Butland's effective temperature has to be increased by 8.6 K. Figure 3 compares the effective temperatures calculated with equations (3) and (4). Results obtained with the phonon density of states of the JEFF-4T1 library lie between these two trends.

3 Perturbation scheme

The integral benchmarks selected in this study are part of the MISTRAL program carried out in the EOLE reactor of CEA Cadarache [12]. A detailed description of the experiments can be found in reference [24]. This program was the subject of the work reported in reference [25], in which the impact of the thermal scattering law of H$_2$O on the isothermal reactivity coefficients α_{iso} is studied. The present work focuses on the integral results measured with the MISTRAL-1 core, which was a homogenous UO$_2$ configuration that serves as a reference for the whole MISTRAL program. The cylindrical core (Fig. 4) consists of a regular lattice using 750 standard PWR fuel pins (3.7% enriched in ^{235}U) in a square pitch of 1.32 cm with 16 guide tubes dedicated to safety rods. The moderation ratio is 1.7 (representative of light water reactor moderation). The reactivity excess was measured as a function of the temperature up to 354 K with a fine temperature step of 5 K. In the MISTRAL-1 configurations, the concentration of the soluble boron was adjusted in the moderator in order to compensate for the reactivity loss due to the temperature increase. The experimental uncertainties of about ±25 pcm mainly come from the kinetic parameters, the measurements of the doubling time and of the boron concentration. In comparison, the technological
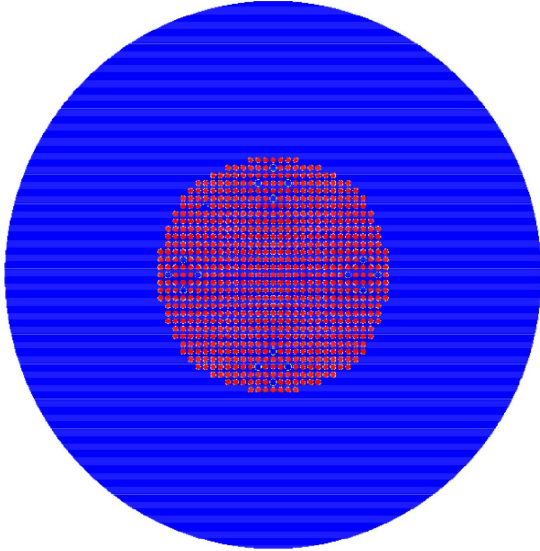
Fig. 4. Radial cross section of the MISTRAL-1 core composed of 750 UOX fuel pins in light water.
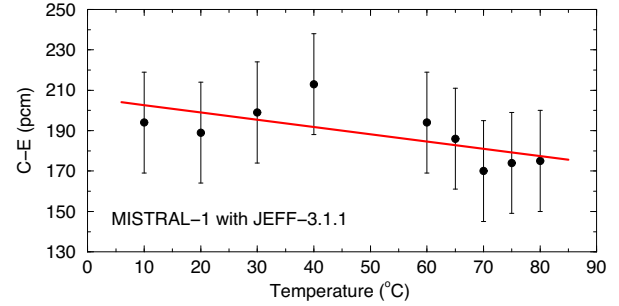

Fig. 5. Differences in reactivity for the MISTRAL-1 core expressed in terms of C-E obtained with the Monte-Carlo code TRIPOLI-4® and the JEFF-3.1.1 library up to 354 K (80°C). The solid line represents the best-fit curve reported in reference [25]. The present calculations account for the thermal expansion of the materials, while in the past study [25], the thermal expansion was taken into account as a correction factor of the Monte-Carlo results. The reported uncertainties only take into account the uncertainties of the kinetic parameters, measurements of the doubling time and boron concentration.

uncertainties are close ± 250 pcm. Results calculated with the Monte-Carlo code TRIPOLI-4® are shown in Figure 5 as a function of T. For each configuration the statistical uncertainty due to the Monte-Carlo calculations is lower than ± 5 pcm. The slope of the solid line represents the calculation bias on the reactivity temperature coefficient α_{iso}. For JEFF-3.1.1, its value is close to -0.36 pcm/K, which remains in the lower limit of the experimental uncertainties (± 0.3 pcm/K).

As indicated by Figure 5, a small variation of the C-E values is expected between the room temperature and 354 K. Such a small variation in conjunction with a demanding computational time makes an uncertainty analysis via repetitive Monte-Carlo perturbations difficult. Therefore, the uncertainty analysis will be performed by direct perturbations of the parameters involved in the thermal scattering law models. In addition, we will limit ourselves to two extreme temperatures at 294 K and 354 K.

Two types of model parameters can be distinguished. Those that are linked to the neutron-nucleus interaction and those that depend explicitly on the studied material. The neutron scattering lengths or equivalently the neutron elastic scattering cross sections at zero Kelvin are well documented in the literature. Their direct perturbation does not cause any problems. By contrast, the range of variation of the parameters describing the temperature-dependent dynamic structure factors for H_2O and UO_2 is poorly known. A solution to overcome this lack of information has been investigated in reference [2]. The reported results indicate that the sources of uncertainties impacting the calculated k_{eff} can be lumped into a single parameter which is the energy interval δ used to reconstruct the phonon density of state. This approximation was successfully used by Rochman on criticality benchmarks [7]. However, it supposes that the other parameters which drive the intramolecular vibrations or H-bond modes have negligible contributions to the k_{eff} uncertainty. This assumption

was also confirmed by Maul in his work on the OPALE reactor [4], but cannot be generalized, especially for well-thermalized neutron spectrum or cold neutron sources. The aim of our perturbation scheme is to apply a scaling factor Δ to this energy interval δ as follows:

$$e_k = \Delta k \delta, \tag{5}$$

and to use Δ as an intermediate parameter for propagating T_{eff} uncertainties to neutron cross sections and k_{eff} values via equation (1). Final results will be summarized in terms of calculation biases expressed in pcm/K.

4 Results and discussions

4.1 Uncertainties on the thermal scattering laws for H_2O

The covariance matrices associated with the thermal scattering laws of H_2O were evaluated in the framework of a few studies [1,2,4–6] in the case of the evaluations available in the JEFF-3.1.1 and ENDF/B.VIII.0 libraries. Although different methodologies were used, they all converged to the same conclusions. At room temperature, the relative uncertainty on the total cross-section of H_2O is lower than 0.5% in the eV energy range and remains below 5% around the thermal energy (25.3 meV). The relative uncertainties start to increase well beyond 5% in the cold and ultra-cold neutron energy ranges, where the translational diffusion behaviour of the water molecule plays a major role in the calculation of the dynamic structure factor. The assessment of the uncertainties at elevated temperatures is less documented because of the lack of accurate experimental values. Fortunately, a recent experimental program carried out at the Vesuvio facility of ISIS (UK) provided a unique set of accurate data for water at 283, 293 and 353 K [26].

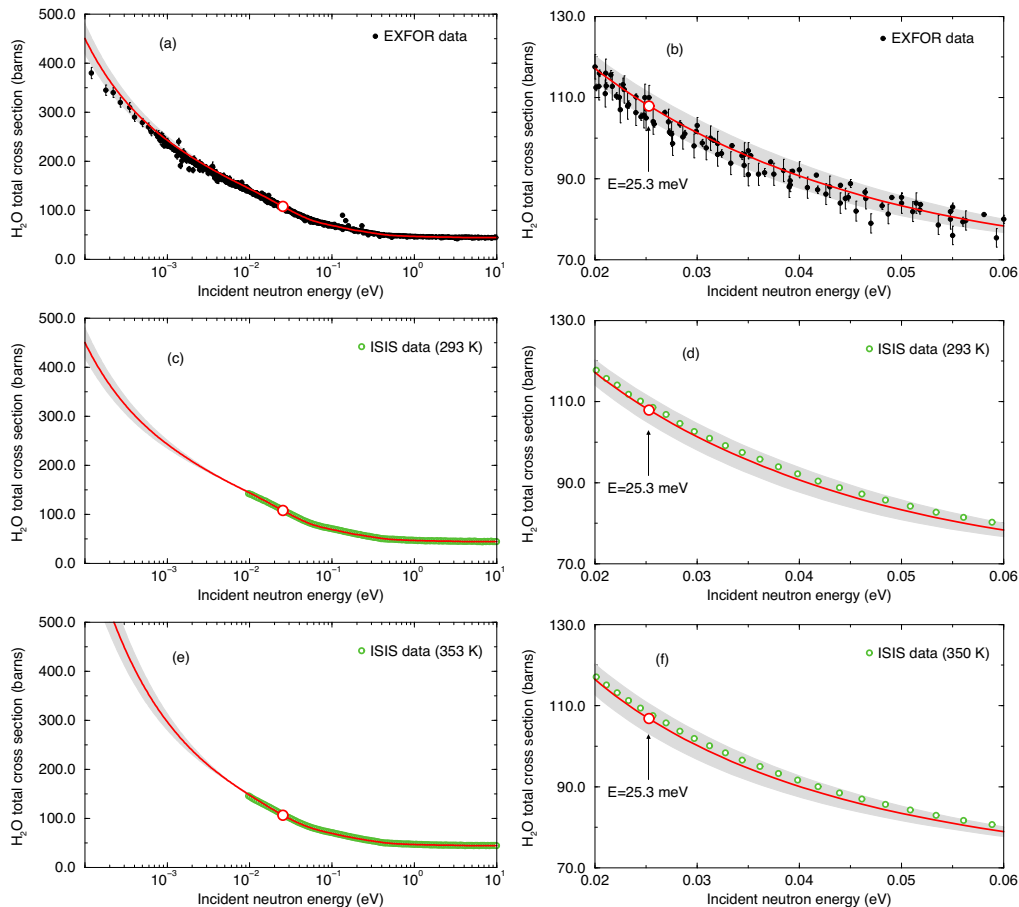Figure 6 summarizes the agreement between the total experimental cross-sections of H_2O and the JEFF-4T1

Fig. 6. Comparison of the experimental and theoretical total cross section of H_2O. For clarity, the EXFOR data [27] and the ISIS data [26] measured at room temperature are shown separately. The grey zones represent the uncertainties.

library. At room temperature, many experimental values are available in the EXFOR data base [27]. The theoretical curve starts to deviate from the data below 1 meV. The right-hand plots of Figure 6 highlight the excellent agreement between the theory and the ISIS data in the thermal energy range. This good agreement validates the position, and the shape of the broad libration band observed in the phonon density of states of H_2O calculated by molecular dynamic simulations. The accuracy of the ISIS data also reveals systematic biases in some of the EXFOR data. This trend is confirmed by the two structures observed in Figure 7, which compares the distributions of the EXFOR and ISIS data with respect to JEFF-4T1.

As introduced in Section 3, covariance matrices for H_2O at 294 and 354 K can be established by direct perturbations of two model parameters. In the eV energy range, the behaviour of the total cross-section mainly depends on the elastic scattering cross section of ^1H at zero kelvin σ_s. The uncertainty on this parameter, recommended by the Neutron Data Standard of IAEA [28], is close to 0.2%:

$$\sigma_s = 20.436\,(41)\ \text{barns}.$$

We decided to apply a direct perturbation of the same order of magnitude, which is equivalent to a perturbation of 41 mbarns on σ_s. In the thermal energy range, the

behaviour of the total cross section is driven by the phonon density of states or equivalently by the effective temperature T_{eff} (Eq. (1)). In order to reach a statistically significant convergence of the results, a perturbation of 5 K was applied to T_{eff}. According to our calculation scheme, this perturbation leads to a variation of 3% and 3.7% of the scaling factor Δ (Eq. (5)) at 294 and 354 K, respectively. The perturbation scheme was complemented by an iterative procedure in order to optimize the uncertainty of the effective temperature, given the constraint to obtain an uncertainty on the thermal total cross section σ_{th} that reproduces the standard deviation of the EXFOR data between 0.02 and 0.06 eV. The following sets of effective temperatures were found:

$$T_{\text{eff}}(294\,\text{K}) = 1195\,(20)\,\text{K},$$

and

$$T_{\text{eff}}(354\,\text{K}) = 1208\,(19)\,\text{K}.$$

In Figure 6, the grey zones represent the resulting uncertainty bands calculated over the full neutron energy range. Around 5 eV, the relative uncertainty is close to 0.2%. In the thermal energy range, the uncertainty increases up to 3% and reaches 10% below 0.1 meV. At 25.3 meV, we
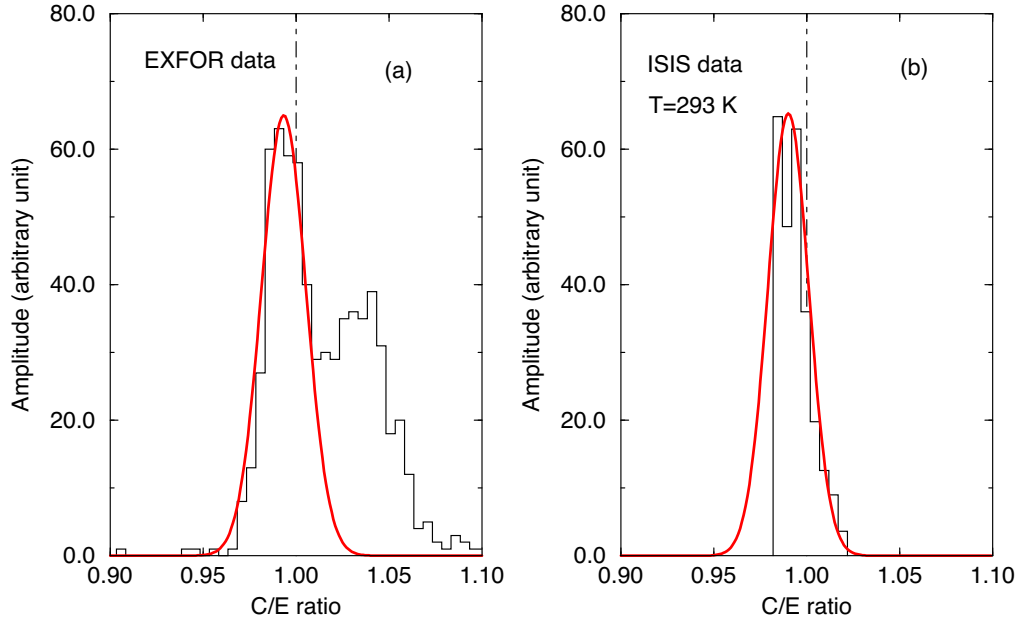
Fig. 7. Distributions of the ratios of the theoretical total cross-section of H_2O (C) to the experimental data (E). The theoretical curves were calculated with the JEFF-4T1 evaluation of H_2O.
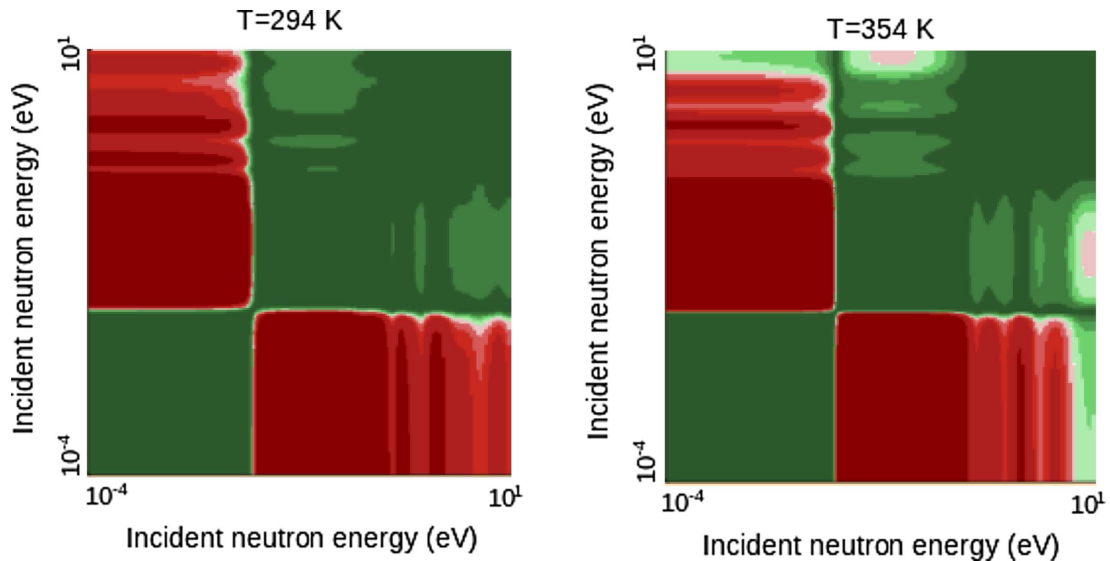

Fig. 8. Correlation matrices of the total cross section of H_2O calculated at 294 and 354 K.

obtained:

$$\sigma_{th}(294\,K) = 108.0\,(32)\ \text{barns},$$

and

$$\sigma_{th}(354\,K) = 106.8\,(37)\ \text{barns}.$$

The correlation matrices associated with the total cross-section of H_2O at 294 and 354 K are shown in Figure 8. Our perturbation scheme provides matrices with a two-block structure which is consistent with previous studies reported in the literature [4].

4.2 Uncertainties on the thermal scattering laws for UO₂

Evaluation works on UO_2 are scarce in the literature. Despite the latest studies performed in the framework of the US library (ENDF/B.VIII.0) [29], no uncertainty analysis on the thermal scattering laws was undertaken. One reason can be the lack of experimental data covering the low neutron energy range. Only two rather old experimental total cross-sections of UO_2 are available in the EXFOR library. In Figure 9, the comparison with the theoretical curve seems to confirm the poor quality of the existing data around thermal energy, making them unreliable
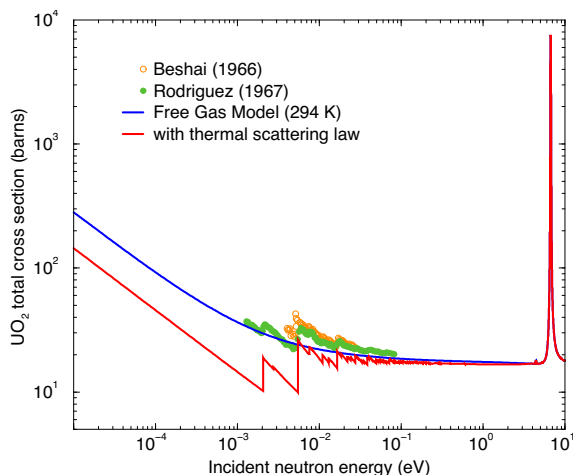
Fig. 9. Comparison of the experimental and theoretical total cross section of UO$_2$ at room temperature.

for uncertainty analysis. Consequently, results provided in this work only comes from roughly estimated prior model parameter uncertainties.

The model parameters of interest are still the effective temperature as well as the neutron scattering lengths b_{coh} associated with the reactions $n+^{16}$O and $n+^{238}$U. Values for b_{coh} were taken from the compilation reported in reference [30], and the order of magnitude of the uncertainty was derived from values reported by Mughaghab [31]:

$$b_{coh}(^{16}O) = 5.803\,(10)\,\text{fm},$$
$$b_{coh}(^{238}U) = 8.402\,(10)\,\text{fm}.$$

For the effective temperature, the difference between the prescriptions of Butland and Meister (Fig. 3) provides a confidence range of variation of T_{eff} for ^{238}U. A conservative estimate of ±10 K was used in this work:

$$T_{eff}(294\,K) = 311\,(10)\,K$$
$$T_{eff}(354\,K) = 369\,(10)\,K.$$

Figure 10 shows the uncertainty band calculated for the UO$_2$ elastic scattering cross-section by applying a perturbation of 0.01 fm and 5 K on b_{coh} and T_{eff}, respectively. The perturbation of the effective temperature of ^{238}U leads to a non-negligible variation of the scaling factor Δ (Eq. (5)) ranging from 10% to 15% at 294 and 354 K, respectively. This perturbation was simultaneously applied to the partial phonon density of states of ^{238}U and ^{16}O in UO$_2$. The relative uncertainty as a function of the incident neutron energy is shown in Figure 11. A reliable value of $\pm1.9\%$ is obtained at the cut-off energy of 4 eV. The uncertainty at the thermal energy slightly increases from $\pm3.9\%$ to $\pm4.8\%$ with the temperature:

$$\sigma_{th}(294\,K) = 15.71\,(61)\,\text{barns},$$

and

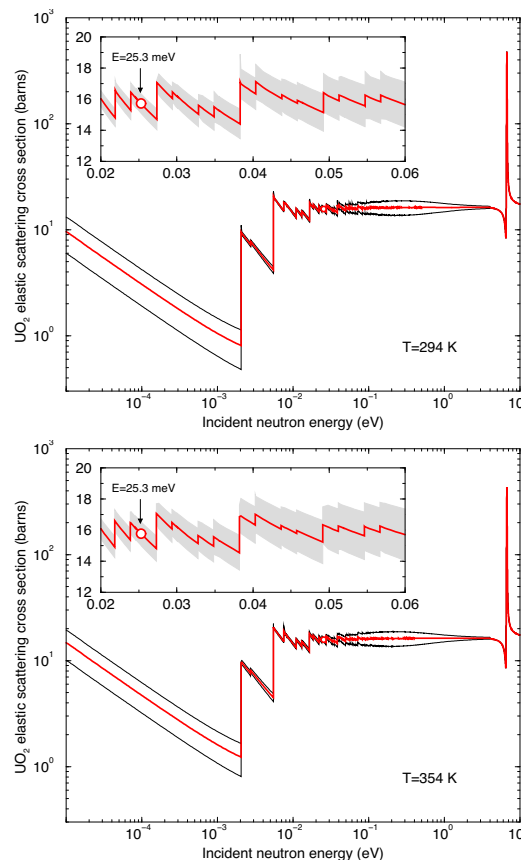$$\sigma_{th}(354\,K) = 15.76\,(76)\,\text{barns}.$$

Fig. 10. Elastic scattering cross sections of UO$_2$ calculated at 294 and 354 K with the JEFF-4T1 evaluations. The solid black lines and the grey zones represent the uncertainties.
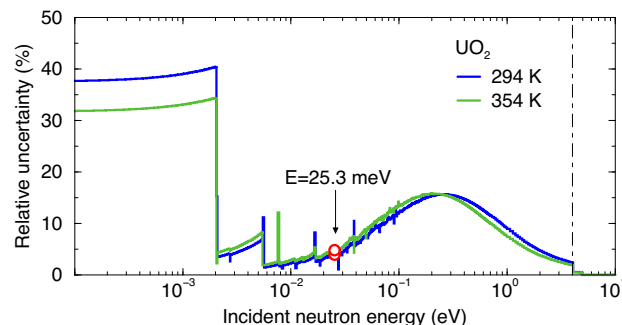

Fig. 11. Relative uncertainty calculated on the elastic scattering cross sections of UO$_2$. The dotted black line indicates the thermal cut-off energy (4 eV).

4.3 Uncertainty on the multiplication factor k_{eff}

This work aims to illustrate the use of the effective temperature as an uncertainty indicator for quantifying the impact of the thermal scattering laws on the neutron multiplication factor. The nominal calculations are performed with the JEFF-3.1.1 library and compared to calculations in which the H$_2$O or UO$_2$ evaluations of the test library JEFF-4T1 are perturbed. The propagation of the model parameter uncertainties to the neutron multiplication

Table 2. Model parameters and uncertainties used in this work.

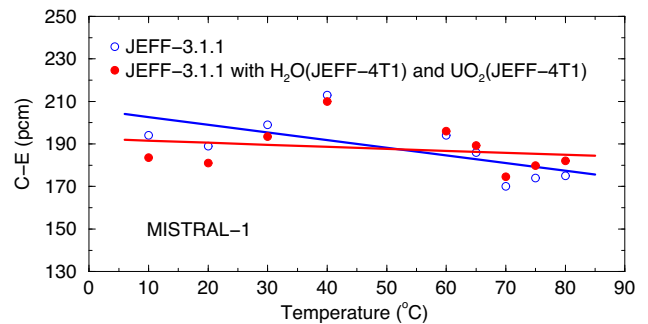| Parameter		294 K	354 K
^{1}H elastic scattering cross section	σ_s	20.436 (41) barns	20.436 (41) barns
Effective temperature ^{1}H in H_2O	T_{eff}	1195 (20) K	1208 (19) K
Bound neutron scattering length of ^{16}O	b_{coh}	5.803 (10) fm	5.803 (10) fm
Bound neutron scattering length of ^{238}U	b_{coh}	8.402 (10) fm	8.402 (10) fm
Effective temperature ^{238}U in UO_2	T_{eff}	311 (10) K	369 (10) K

Table 3. Differences between the calculated (C) and experimental (E) reactivities obtained for the MISTRAL-1 core with the Monte-Carlo code TRIPOLI-4®. The digits in parentheses are the statistical uncertainty due to the Monte-Carlo calculations.

Test case	Test library	294 K		354 K	
		C-E	$(1) - (i)$	C-E	$(1) - (i)$
$i = 1$	JEFF-3.1.1	+189 (1) pcm	–	+175 (1) pcm	–
$i = 2$	JEFF-3.1.1 and H_2O of JEFF-4T1	+198 (5) pcm	+9 pcm	+198 (3) pcm	+23 pcm
$i = 3$	JEFF-3.1.1 and UO_2 of JEFF-4T1	+172 (3) pcm	−17 pcm	+160 (3) pcm	−16 pcm

factor of the MISTRAL-1 program follows the same methodology as presented in Sections 4.1 and 4.2. The parameters and uncertainties used in this study are summarized in Table 2. We applied perturbations of 5 K to T_{eff}, 41 mbarns to σ_s and 0.01 fm to b_{coh}.

The nominal results calculated with TRIPOLI-4® before perturbation are compared in Table 3 with those obtained thanks to the JEFF-4T1 evaluations of H_2O and UO_2. The thermal scattering laws of H_2O and UO_2 coming from JEFF-4T1 have opposite effects on k_{eff}. The compensation of each contribution is illustrated with the C-E results reported in Figure 12. The calculation bias on the isothermal reactivity coefficients α_{iso}, given by the slope of the solid line, is improved with the JEFF-4T1 library. It becomes equal to -0.09 pcm/K, compared to -0.36 pcm/K with JEFF-3.1.1. Such an improvement is reflected by the low uncertainty on the k_{eff} values reported in Table 4. The uncertainties due to the thermal scattering laws of H_2O are close to ± 50 pcm, and those due to UO_2 remain lower than 30 pcm. For comparison, Table 5 shows results previously reported in the literature for the MITRAL-1 core. The non-negligible uncertainties associated with the thermal scattering laws of H_2O in JEFF-3.1.1 (>100 pcm) progressively decrease to the present results. This trend is explained by the intense work performed on the modelization of the dynamical structure factor of H_2O and on the total cross-section measurements at elevated temperatures.

The results of Table 4 can be conveniently translated into pcm/K. This uncertainty indicator represents a calculation bias on k_{eff} relatively to the effective temperature uncertainty. In our case, it has the advantage of providing rather similar results for H_2O and UO_2. At room temperature, it is close to 2.6 pcm/K on average for both H_2O and UO_2, while it is dominated by H_2O at elevated

Fig. 12. Differences in reactivity for the MISTRAL-1 core obtained with TRIPOLI-4®. The solid blue line is the best-fit curve obtained with the JEFF-3.1.1 library alone (see Fig. 5). The solid red line is the best-fit curve obtained when the thermal scattering laws of H_2O and UO_2 are replaced by those of JEFF-4T1. The slope of each line gives the calculation bias on the isothermal reactivity temperature coefficient α_{iso}. For clarity, the uncertainties are shortly discussed in Section 3 and not reported in the plot.

temperatures. Consequently, an average estimate of about 2.3 pcm/K can be safely used from 294 to 354 K. This estimate provides a k_{eff} uncertainty of ± 51 pcm, resulting from the quadratic sum of each contribution given effective temperature uncertainties of ± 20 K and ± 10 K for H_2O and UO_2, respectively. The consistency of the obtained results over the studied temperature range can be seen as a step forward to store thermal scattering law uncertainties in evaluated nuclear data files. Providing uncertainties on the effective temperatures instead of covariance matrices associated to temperature-dependent phonon densities of states can be easily handle in a modern nuclear data format [32].

Table 4. k_{eff} uncertainties obtained for the MISTRAL-1 core at 294 and 354 K due to the model parameter uncertainties reported in Table 2. This uncertainty indicator expressed in pcm/K represents a calculation bias on k_{eff} relatively to the effective temperature uncertainty. The digits in parentheses come from the statistical uncertainty due to the Monte-Carlo calculations.

Test case	Thermal Scattering laws	294 K		354 K	
		Δk_{eff}	calculation bias	Δk_{eff}	calculation bias
$i = 1$	H_2O	$\pm 50\,(6)$ pcm	± 2.5 pcm/K	$\pm 56\,(3)$ pcm	± 2.9 pcm/K
$i = 2$	UO_2	$\pm 27\,(3)$ pcm	± 2.7 pcm/K	$\pm 12\,(3)$ pcm	± 1.2 pcm/K

Table 5. Evolution of the k_{eff} uncertainties for the MISTRAL-1 core at 294 and 354 K due to the thermal scattering laws of H_2O.

Author	H_2O evaluation	294 K	354 K
Noguere [2]	H_2O evaluation from JEFF-3.1.1	± 130 pcm	± 137 pcm
Scotta [5]	H_2O evaluation from CAB model using EXFOR data	± 71 pcm	± 155 pcm
This work	H_2O evaluation from JEFF-4T1 using EXFOR and ISIS data	± 50 pcm	± 56 pcm

The major conclusion of this study is that in the future evaluated nuclear data libraries, uncertainty budget analysis associated with the low neutron energy scattering process of H_2O and UO_2 will be a marginal contribution compared to the uncertainties on the capture process. Indeed, uncertainties in the UOX reactivity due to the $^1H(n,\gamma)$ and $^{238}U(n,\gamma)$ reactions are expected to be as large as ± 150 pcm, if the covariance database COMAC [33] is used in the calculations.

5 Conclusions

The propagation of the model parameter uncertainties involved in the description of the thermal scattering law of H_2O to neutronic parameters is the subject of a few works reported in the literature. The present uncertainty analysis provides new results as a function of the temperature for H_2O and complements past uncertainty analysis with UO_2. The obtained results confirm that the accuracy of the latest evaluations of H_2O and UO_2, available in the working library labelled JEFF-4T1, will imply a modest impact of about ± 50 pcm on the k_{eff} uncertainty of UOX benchmarks. In comparison to capture reactions, the low neutron energy scattering process will become a marginal source of uncertainties. This achievement can be explained by the intense works performed on the modelization of the dynamical structure factor of H_2O and UO_2 in association with new measurements performed at elevated temperatures. This conclusion is only valid for UOX benchmarks and cannot be generalized, especially for well-thermalized neutron spectrum or cold neutron sources.

The results reported in this work also probe that the specificity of the neutron spectrum for UOX cores makes it possible to use the effective temperature as an uncertainty indicator to quantify the impact of the thermal scattering laws on the calculated reactivity. The corresponding uncertainty indicator, expressed in pcm/K, represents a calculation bias on k_{eff} relatively to the effective temperature uncertainty. In the framework of the MISTRAL-1 program, it has the advantage to be close to 2.3 pcm/K on average for both H_2O and UO_2 contributions. This approach simplifies the relationship between the condensed matter and neutronic physics, and reduces the complexity of the uncertainty analysis to a single parameter. Therefore, providing uncertainties about the effective temperatures in the evaluated nuclear data files is a recommendation that could avoid dealing with the covariance matrices associated to the temperature-dependent phonon densities of states.

Conflict of interests

The authors declare that they have no competing interests to report.

Data availability statement

This article has no associated data generated and/or analyzed.

Author contribution statement

G. Noguere: conceptualization, methodology, software, validation, writing, review, editing, visualization. S. Xu: software, review, editing.

References

1. D. Rochman, A. Koning, Nucl. Sci. Eng. **172**, 287 (2012)
2. G. Noguere et al., Ann. Nucl. Energy **104**, 132 (2017)
3. J.P. Scotta et al., EPJ Web of Conf. **146**, 13010 (2017)
4. L. Maul et al., Ann. Nucl. Energy **121**, 232 (2018)
5. J.P. Scotta et al., EPJ Nuclear Sci. Technol. **4**, 32 (2018)
6. C.W. Chapman et al., Nucl. Sci. Eng. **195**, 13 (2021)
7. D. Rochman et al., EPJ Nuclear Sci. Technol. **8**, 3 (2022)
8. W.E. Lamb, Phys. Rev. **55**, 190 (1939)
9. G.M. Borgonovi, *Neutron Scattering Kernels Calculations at Epithermal Energies*, Technical Report GA-9950, Gulf General Atomic, San Diego, USA, (1970)
10. T.M. Sutton et al., Comparison of some Monte Carlo models for bound hydrogen scattering, in *Proc. Int. Conf. on Mathematics, Computational Methods and Reactor Physics, Saratoga Springs*, New York USA (2009)
11. J. Dawidowski et al., Ann. Nucl. Energy **90**, 247 (2016)
12. S. Cathalau et al., MISTRAL: an experimental program in the EOLE facility devoted to 100% MOX core physics, in *Proc. Int. Conf. on Physics of Reactors PHYSOR*, Mito, Japan (1996)
13. E. Brun et al., Ann. Nucl. Energy **82**, 151 (2015)
14. A. Plompen et al., Status and perspective of the development of JEFF-4, in *Proc. Int. Conf. Nuclear Data for Sci. and Technol.*, Gather Town (2022)
15. J.I. Marquez Damian et al., Ann. Nucl. Energy **65**, 280 (2014)
16. G. Noguere et al., Phys. Rev. B **102**, 134312 (2020)
17. S. Xu et al., Nucl. Instrum. Methods Phys. Res., Sect. A **1002**, 165251 (2021)
18. S. Xu, G. Noguere, EPJ Nuclear Sci. Technol. **8**, 8 (2022)
19. R. Macfarlane et al., *The NJOY Nuclear Data Processing System Version 2016, Report LA-UR-17-20093* (Los Alamos National Laboratory, USA, 2017)
20. A.T.D. Butland, Ann. Nucl. Sci. Eng. **1**, 575 (1974)
21. G.R. Stewart, Rev. Sci. Instrum. **54**, 1 (1983)
22. A. Meister, A. Santamarina, The effective temperature for Doppler broadening of neutron resonances in UO_2, in *Proc. Int. Conf. on Physics of Reactors PHYSOR*, Long Island, USA (1998)
23. A. Meister et al., *Measurements to Investigate the Doppler-Broadening of ^{238}U Neutron Resonances, Report IRMM-GE/R/ND/01/96* (Institute for Reference Materials and Measurements, Belgium, 1996)
24. L. Erradi et al., Nucl. Sci. Eng. **144**, 47 (2003)
25. J.P. Scotta et al., EPJ Nuclear Sci. Technol. **2**, 28 (2016)
26. J.I. Marquez Damian et al., EPJ Web Conf. **239**, 14001 (2020)
27. N. Otuka et al., Nucl. Data Sheets **120**, 272 (2014)
28. A.D. Carlson et al., Nucl. Data Sheets **148**, 143 (2018)
29. J.L. Wormald et al., Nucl. Sci. Eng. **195**, 227 (2021)
30. V.F. Sears, Neutron News **3**, 29 (1992)
31. S.F. Mughabghab, *Atlas of Neutron Resonances*, 6th edn. (Elsevier, 2018)
32. Specifications for the generalised nuclear database structure, OECD/NEA report no. 7519 (2020)
33. P. Archier et al., COMAC: nuclear data covariance matrices library for reactor applications, in *Proc. Int. Conf. on Physics of Reactors PHYSOR*, Kyoto, Japan, (2014)